Supporting Information

Synergistic action of spatially self-reconfiguring bilayer lithiophilic alloys and inorganic passivation layers for enhancing Li metal anode performance

Yiwei Bu,[a] Shidi Huang [b,*], Jinqi Zhu,[a] Zhe Cui,[a] Mengluan Gao,[a] Wenqing Wang, [a] Rujia Zou [a,*]

[a] State Key Laboratory for Modification of Chemical Fibers and Polymer Materials, College of Materials Science and Engineering, Donghua University, Shanghai 201620, China

E-mail: rjzou@dhu.edu.cn

[b] School of Ecological Technology and Engineering, Shanghai Institute of Technology, Shanghai 201418, P. R. China

E-mail: sdhuang@sit.edu.cn

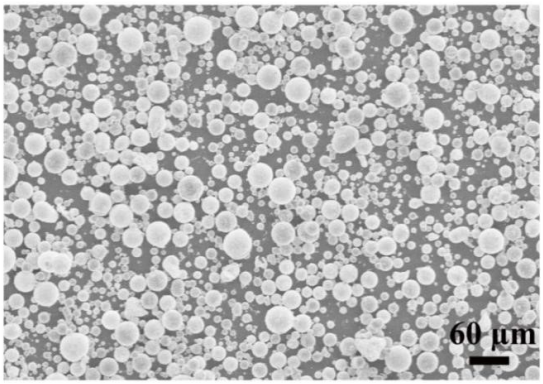

Figure S1 SEM image of Mg-Zn alloy particles synthesized by atomization method.

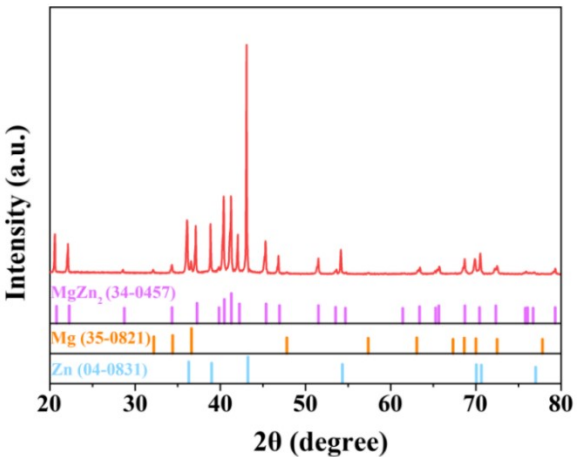

Figure S2 XRD pattern of Mg-Zn alloy particles synthesized by atomization method.

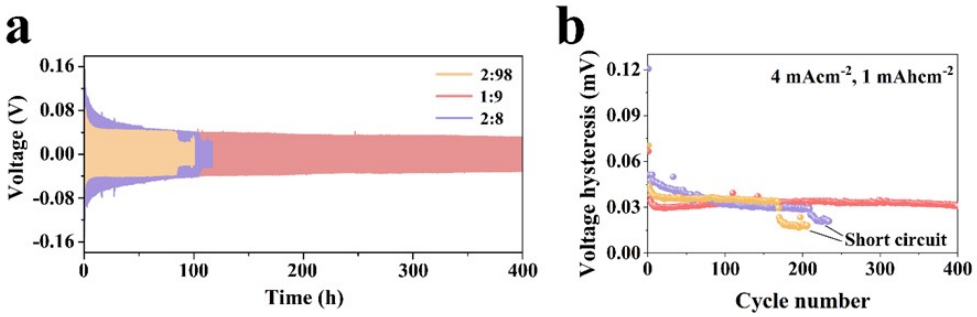

Figure S3 (a) Galvanostatic discharge/charge voltage profiles and (b) average hysteresis of LMZG electrodes composed of alloys with Mg/Zn weight ratios of 2:98, 10:90, and 20:80, respectively, at 4 mA cm^{-2} for 1 mAh cm^{-2}.

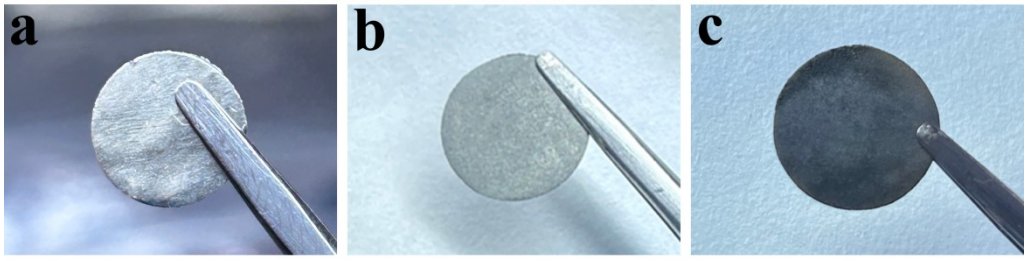

Figure S4 The digital photographs of (a) bare Li electrode, (b) LMZ electrode, and (c) LMZG electrode.

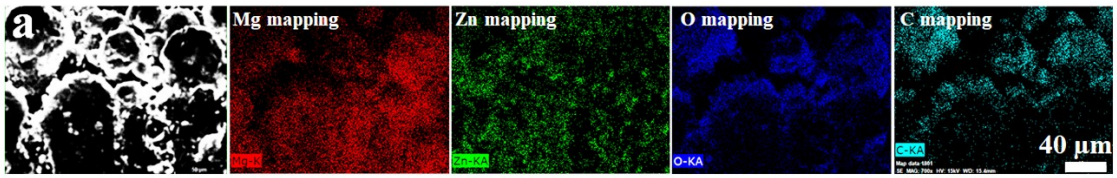

Figure S5 Cross-sectional SEM and EDS images of LMZG electrode before cycle.

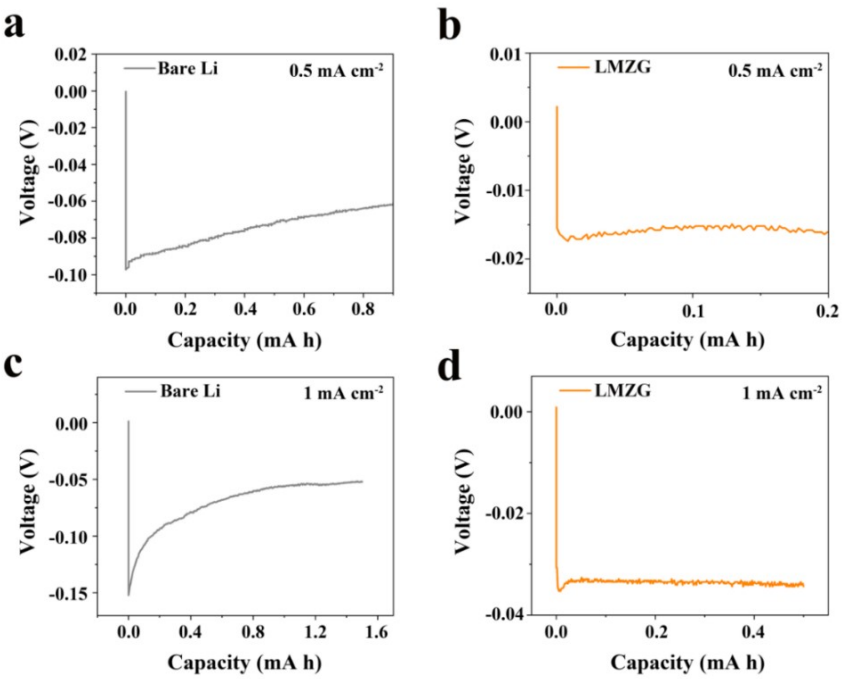

Figure S6 Voltage profiles of (a) bare Li and (b) LMZG electrode upon discharging at 0.5 mA cm^{-2} for 0.5 mAh cm^{-2}. Voltage profiles of (c) bare Li and (d) LMZG electrode upon discharging at 1 mA cm^{-2} for 1 mAh cm^{-2}.

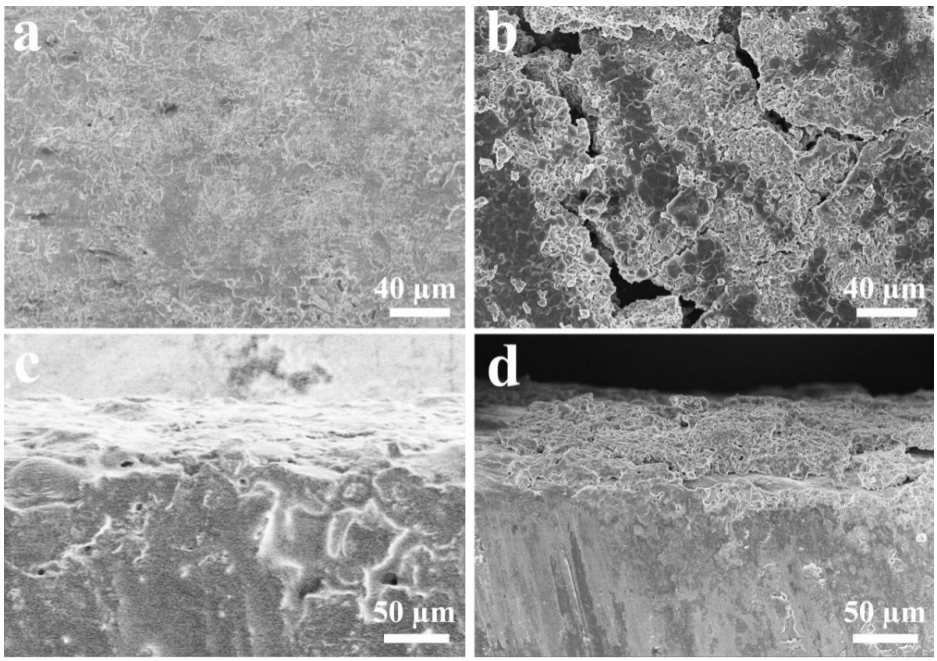

Figure S7 (a) Top-view and (c) cross-sectional SEM images of LMZG electrode after 50 cycles at 1 mA cm^{-2} for 1 mAh cm^{-2}; (b) Top-view and (d) cross-sectional SEM images of bare Li electrode after 50 cycles at 1 mA cm^{-2} for 1 mAh cm^{-2}.

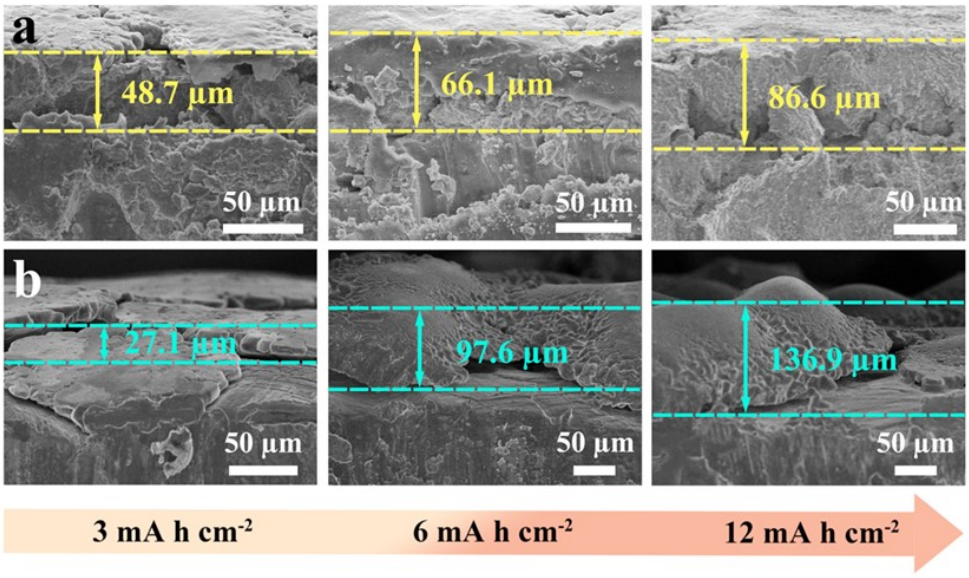

Figure S8 Side-view SEM images of 3, 6, and 12 mAh cm^{-2} deposited at a current of 1 mA cm^{-2} after 10 cycles of depositing 1 mAh cm^{-2} at a current of 1 mA cm^{-2}: (a) LMZG electrode and (b) Bare Li electrode.

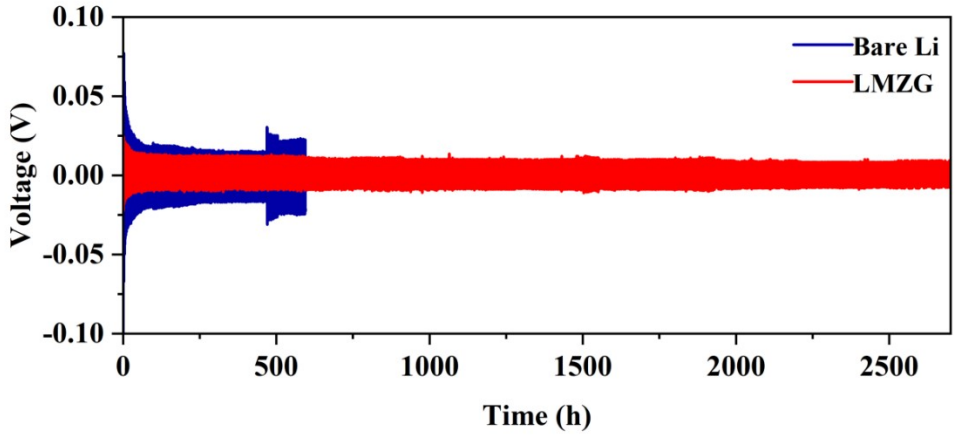

Figure S9 Galvanostatic discharge/charge voltage profiles of LMZG and bare Li in symmetric cells at 0.5 mA cm^{-2} for 0.5 mAh cm^{-2}.

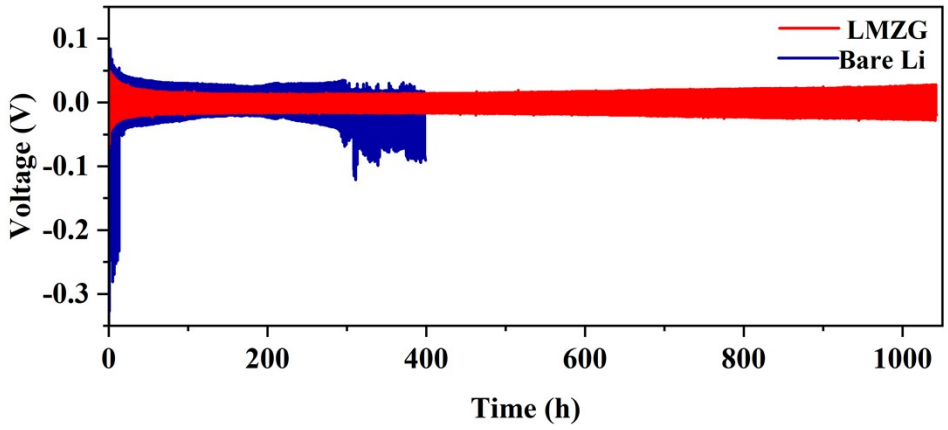

Figure S10 Galvanostatic discharge/charge voltage profiles of LMZG and bare Li in symmetric cells at 2 mA cm^{-2} for 2 mAh cm^{-2}.

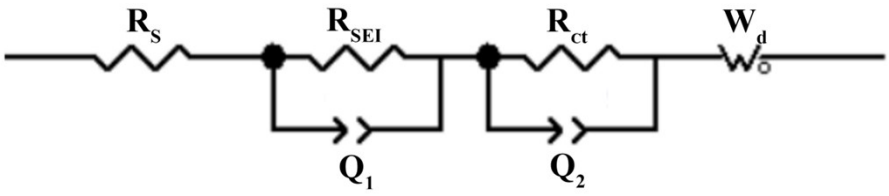

Figure S11 The equivalent circuit for the fitting of EIS spectra of LMZG and bare Li. R_S, R_{SEI}, R_{ct}, Q, and W_d refer to the internal resistance, surface layer resistance, charge transfer resistance, constant phase elements, and Warburg impedance of symmetric cells, respectively.

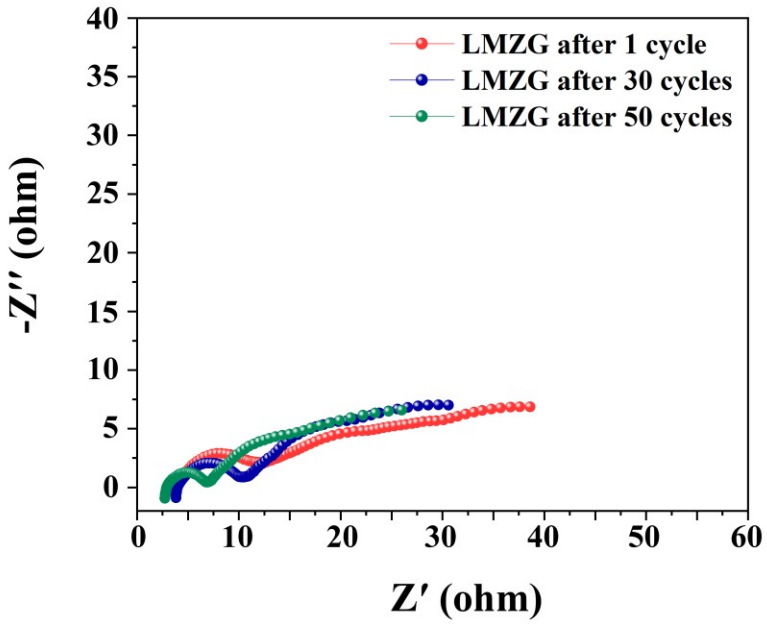

Figure S12 Electrochemical impedance spectra of LMZG electrode in symmetric cells after cycling at 1 mA cm^{-2}.

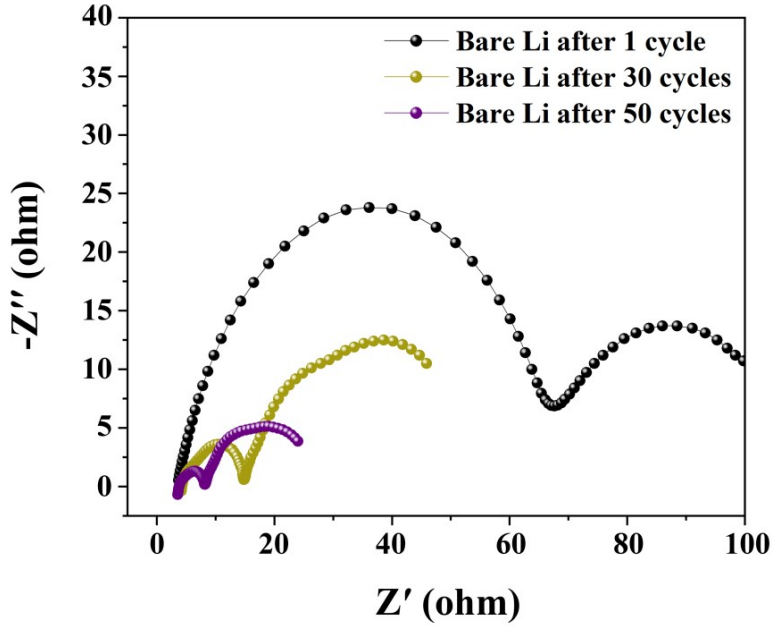

Figure S13 Electrochemical impedance spectra of bare Li electrode in symmetric cells after cycling at 1 mA cm^{-2}.

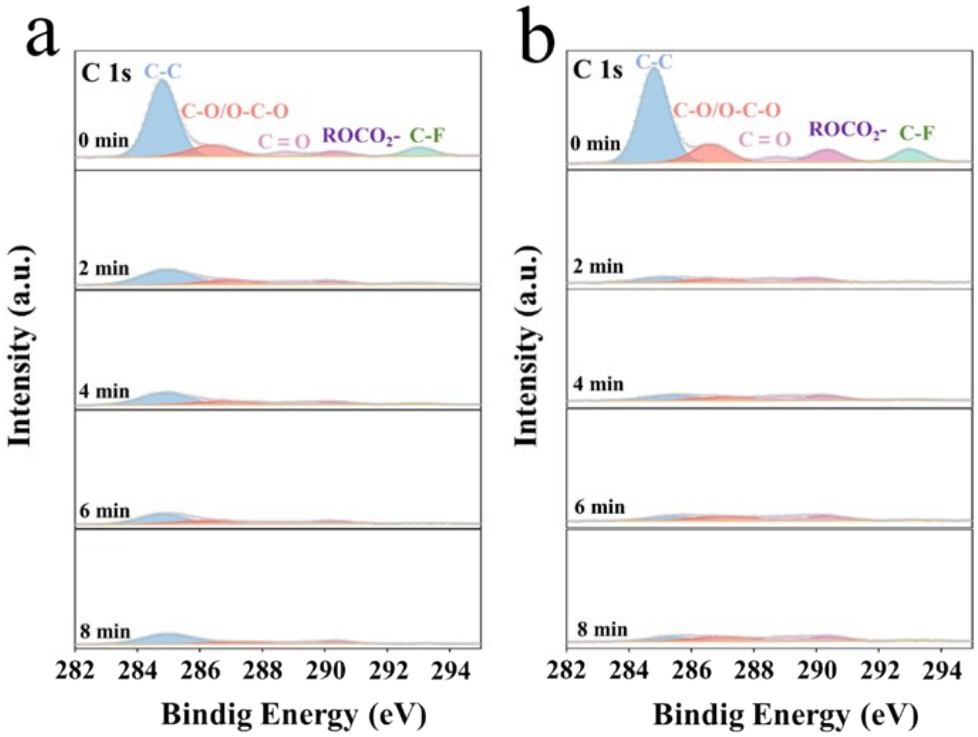

Figure S14 XPS depth profile of (a) LMZG and (b) bare Li electrode after 50 cycles at 1 mA cm^{-2} for 1 mAh cm^{-2}.

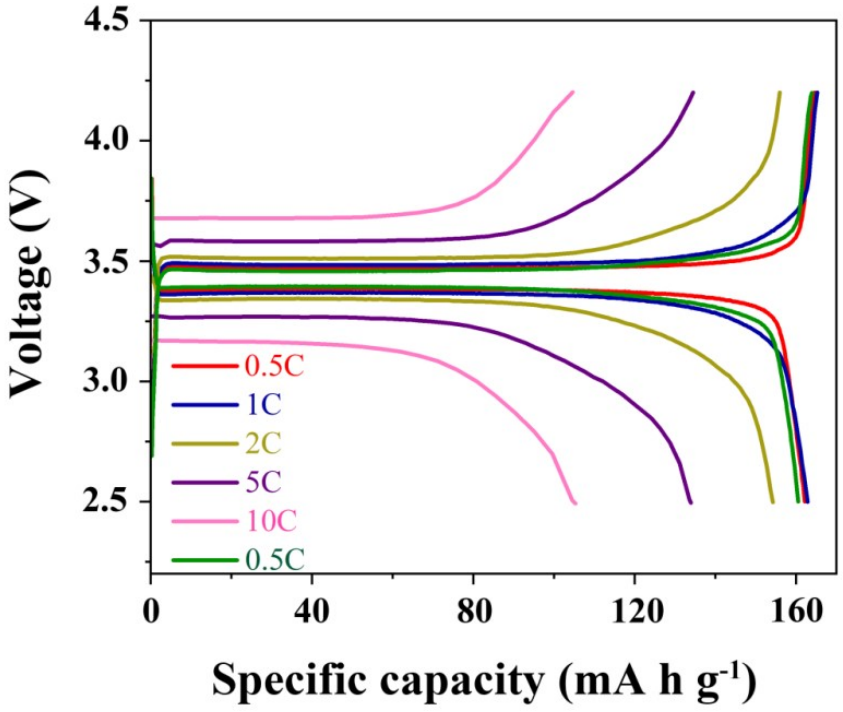

Figure S15 Charge/discharge profiles of bare Li//LFP full cells at various rates.

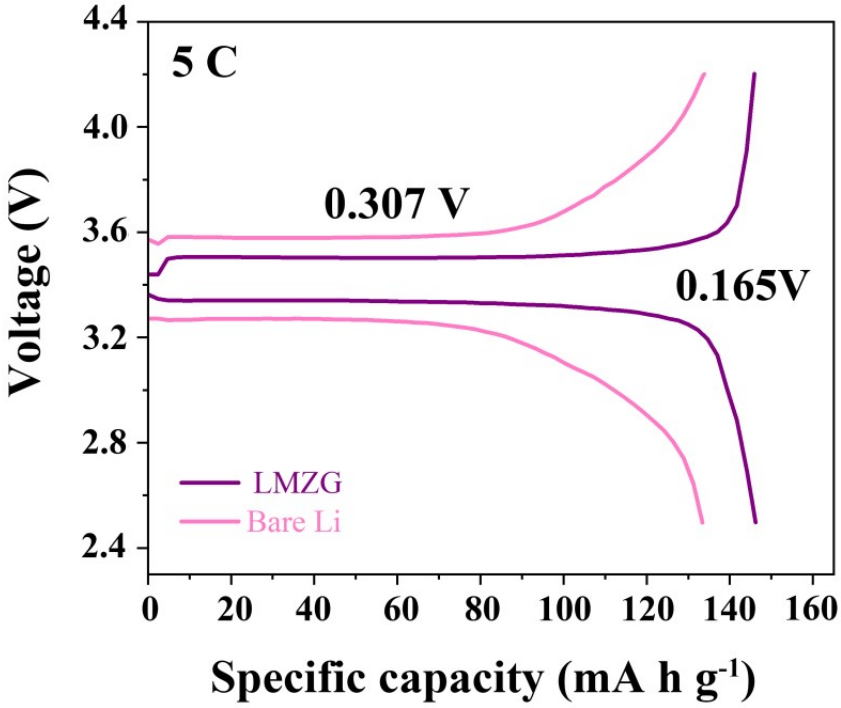

Figure S16 Voltage curves comparison of the LMZG and bare Li full-cells at 5 C.

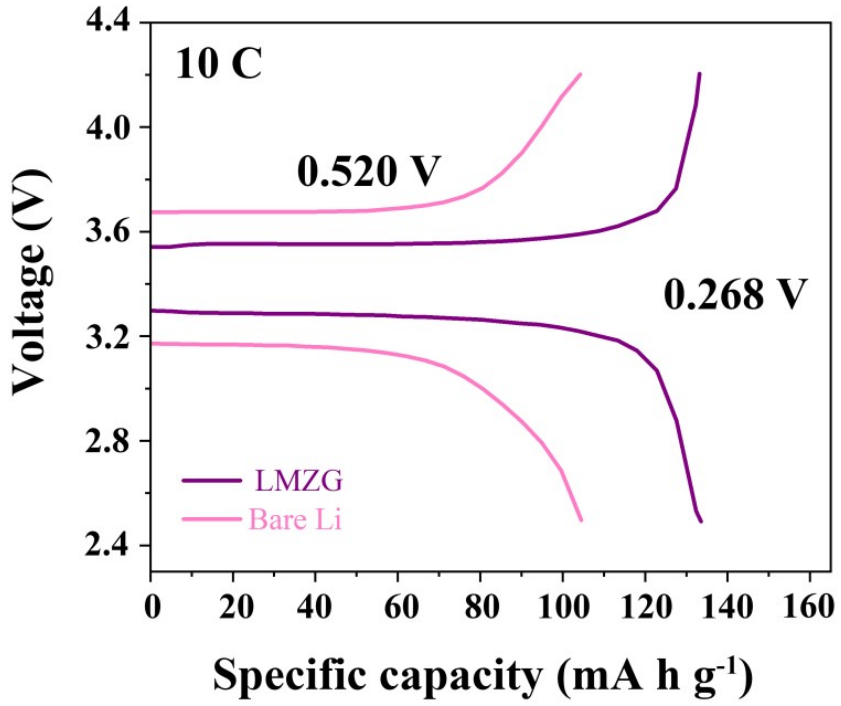

Figure S17 Voltage curves comparison of the LMZG and bare Li full-cells at 10 C.

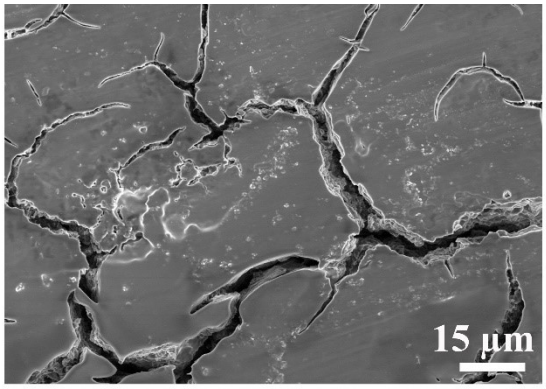

Figure S18 SEM images of bare Li metal anode taken from bare Li//LFP full cells after 400 cycles at 1 C.

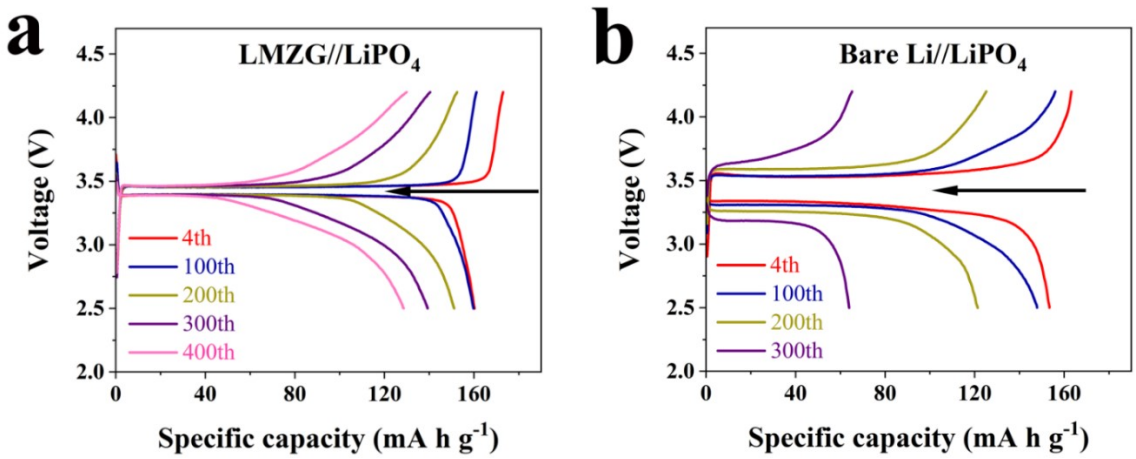

Figure S19 Charge/discharge profiles of (a) LMZG//LFP and (b) bare Li//LFP full cells at 1C.

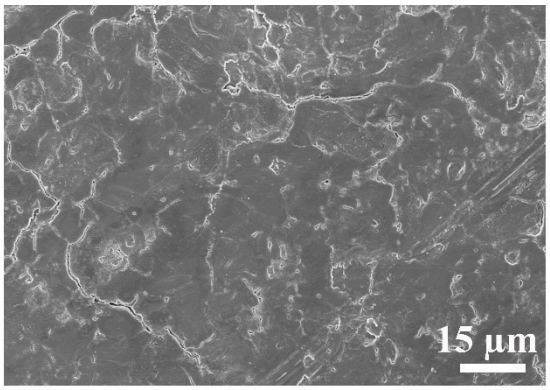

Figure S20 SEM images of LMZG electrode taken from LMZG//LFP full cells after 400 cycles at 1 C.

Table S1 The corresponding fitting values are based on the equivalent circuit.

Electrode	Cycle	$R_S(\Omega)$	$R_{SEI}(\Omega)$	$R_{ct}(\Omega)$
LMZG	1	3.917	6.42	28.7
	30	4.04	6.117	23.69
	50	2.985	3.829	16.19
Bare Li	1	3.653	63.75	39.13
	30	4.408	10.56	40.26
	50	3.977	4.202	18.15